Core Material Design of a High Performance Rotating Machine Considering Magnetic Anisotropy

Atsushi Ikariga*, Masato Enokizono, Hiroyasu Shimoji*** and Hirofumi Yamashiro******

Abstract - This paper deals with a new design method for a small-size rotating machine with high power. In order to achieve high performance, secondary excitation by Nd-Fe-B magnets and the grain-oriented electrical steel sheets were selected and a new design using dual rotors is proposed. The outline of the high-performance rotating machine will be presented and the results of the finite element analysis by using this method combined with the E&SS modeling will be shown in the paper.

Keywords: Material modeling, Finite element method, vector magnetic property and rotating machine

1. Introduction

The designing under high magnetic flux density is necessary to realize high-performance electrical machinery and apparatus. It is important to know how to suitably select and use the magnetic properties of core materials such as electrical steels. Use of the complex characteristics in the magnetic field analysis is important in designing of the electrical machinery of a high performance. Then it is required that the complex characteristics of the magnetic materials are taken into consideration in the magnetic field analysis. The conventional analysis was not able to consider the phase difference between the magnetic flux density B and the magnetic field strength H. Therefore, it was difficult to consider the complex characteristics in the magnetic anisotropy materials.

Recently the measuring technique of the two-dimensional magnetic properties has developed rapidly and the achievements have become a center of attention. The two-dimensional magnetic properties are the relationship between the measured magnetic flux density B and the measured magnetic field strength H as vector quantity. These modelings can express the magnetic anisotropy and iron loss precisely. We have enabled the analysis of the magnetic anisotropy and nonlinearity that have so far been considered difficult to do. Thus the tendency that iron loss increases when the phase difference between B and H occurs, is well expressed in this method. The designing of the high performance rotating machine was carried out by using the magnetic field analysis, combining the finite element method with a new E&SS (Enokizono, Soda & Shimoji) modeling [1]-[3].

* Department of Electrical and Electronic Engineering, Faculty of Engineering, Oita University, 700 Dannoharu, Oita 870-1192, Japan (ikariga@cc.oita-u.ac.jp)
** Department of Electrical and Electronic Engineering, Faculty of Engineering, Oita University, 700 Dannoharu, Oita 870-1192, Japan (enoki@cc.oita-u.ac.jp)
*** Department of Electrical and Electronic Engineering, Faculty of Engineering, Oita University 700 Dannoharu, Oita 870-1192, Japan. (simoji@cc.oita-u.ac.jp)
**** Department of Electrical and Electronic Engineering, Faculty of Engineering, Oita University, 700 Dannoharu, Oita 870-1192, Japan. (yamashiro@mag.eee.oita-u.ac.jp)
Received June 7, 2005 ; Accepted August 23, 2005

2. The Finite Element Method with the E&SS Modeling

2.1 The Representation of Magnetic Anisotropy

Fig. 1 shows an alternating magnetic flux and a rotating magnetic flux. The alternating magnetic flux can be defined by the maximum magnetic flux density B_{max} and the inclination angle θ_B from the easy axis. The rotating magnetic flux can be defined by the axis ratio α and the maximum magnetic flux density B_{max} and the inclination angle θ_B from the easy axis. The easy axis direction and the hard axis direction exist in any magnetic material. The nonlinear magnetic properties of each magnetic flux condition we have used in calculation are obtained by using the two-dimensional magnetic properties measurement [4], [5].

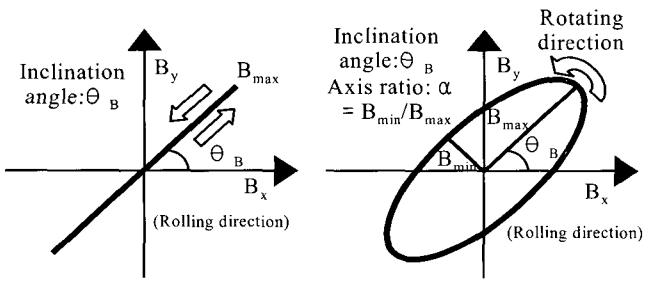

(a) Alternating flux condition (b) Rotating flux condition

Fig. 1 Representation of alternating and rotating flux.

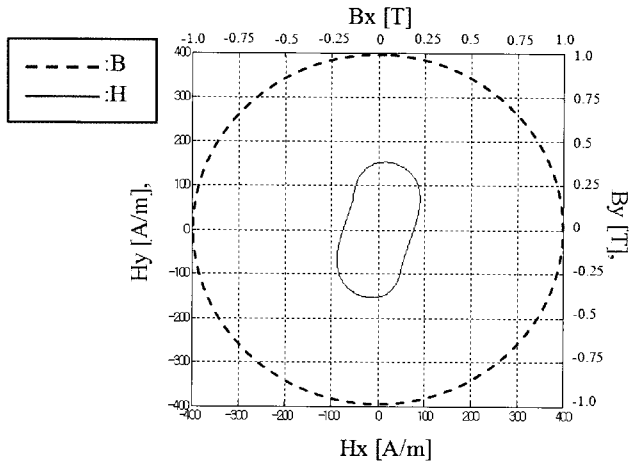

Fig. 2 The magnetic field measured in rotation flux condition(sample: non-oriented electrical steel sheet, α=1, B_{max}=1 [T])

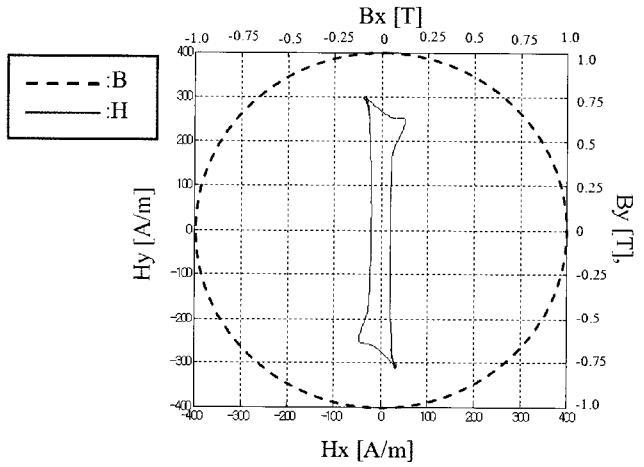

Fig. 3 The magnetic field measured in rotation flux condition(sample: grain-oriented electrical steel sheet, α=1, B_{max}=1 [T])

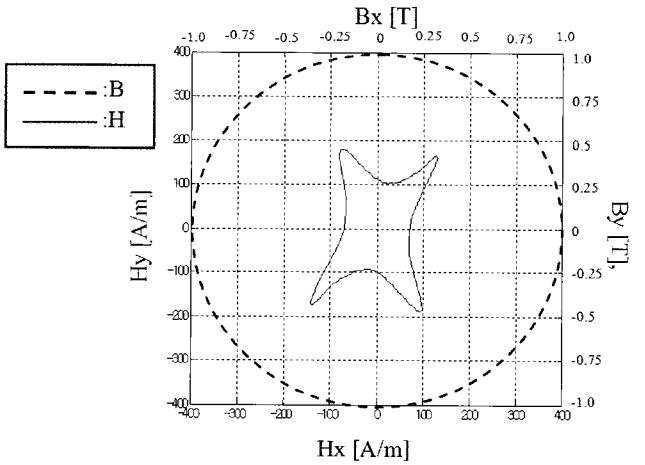

Fig. 4 The magnetic field measured in rotation flux condition(sample: double grain-oriented electrical steel sheet, α=1, B_{max}=1 [T])

For example, Fig. 2 shows the magnetic field loop of a non-oriented electrical steel sheet, which has the hard axis direction near 45 degrees through 120 degrees. Fig. 3 shows the magnetic field loop of a grain-oriented electrical steel sheet having the hard axis direction near 90 degrees. Fig. 4 shows the magnetic field loop of a double grain-oriented electrical steel sheet having the hard axis direction near 45 degrees and 130 degrees.

2.2 The E&SS Modeling

The magnetic flux density B and the magnetic field strength H in anisotropic materials are not parallel when the rotating magnetic field is applied to materials and the alternating magnetic field is applied with θ_B. The magnetic properties have strong nonlinearity as a function of the magnetic flux density and the inclination angle θ_B. The E& SS modeling can express alternating and rotating hysteresis as a relationship between **B** and **H** during one period. The modeling is defined with the following equations.

$$\begin{cases} H_x = \nu_{xr}\left(B_{\max},\theta_B,\alpha,\tau\right)B_x(\tau) \\ \qquad + \nu_{xi}\left(B_{\max},\theta_B,\alpha,\tau\right)\int_0^\tau B_x(\tau)d\tau \\ H_y = \nu_{yr}\left(B_{\max},\theta_B,\alpha,\tau\right)B_y(\tau) \\ \qquad + \nu_{yi}\left(B_{\max},\theta_B,\alpha,\tau\right)\int_0^\tau B_y(\tau)d\tau \end{cases} \quad (1)$$

where ν_{xr} and ν_{yr} are named as the magnetic reluctivity coefficients, and then ν_{xi} and ν_{yi} are named as the magnetic hysteresis coefficients. The magnetic reluctivity coefficients and the magnetic hysteresis coefficients are altered as a waveform in one period.

The variable τ is in a range from zero to 2π. We approximate B-waveforms sinusoidal, and expressed as follows:

$$\begin{cases} B_x = R_{Bx}\cos\tau - I_{Bx}\sin\tau \\ B_y = R_{By}\cos\tau - I_{By}\sin\tau \end{cases} \quad (2)$$

where R_{Bx}, R_{By}, I_{Bx} and I_{By} are coefficients.

The distorted H waveforms can be expressed as the following equation in the Fourier series:

$$\begin{cases} H_x = \sum_{n=1}^{N}\left(R_{(2n-1)Hx}\cos(2n-1)\tau - I_{(2n-1)Hx}\sin(2n-1)\tau\right) \\ H_y = \sum_{n=1}^{N}\left(R_{(2n-1)Hy}\cos(2n-1)\tau - I_{(2n-1)Hy}\sin(2n-1)\tau\right) \end{cases} \quad (3)$$

where R_{Hx}, R_{Hy}, I_{Hx} and I_{Hy} are coefficients.

As a result, the magnetic reluctivity coefficient and the magnetic hysteresis coefficient are given by

$$\begin{cases} v_{xr} = \dfrac{\sum_{n=1}^{N} R_{(2n-1)H_x}\cos(2n-1)\tau}{\cos\tau}\left(\dfrac{R_{B_x}}{R_{B_x}^2+I_{B_x}^2}\right) + \dfrac{\sum_{n=1}^{N} I_{(2n-1)H_x}\sin(2n-1)\tau}{\sin\tau}\left(\dfrac{I_{B_x}}{R_{B_x}^2+I_{B_x}^2}\right) \\ v_{xi} = \dfrac{\sum_{n=1}^{N} R_{(2n-1)H_x}\cos(2n-1)\tau}{\cos\tau}\left(\dfrac{I_{B_x}}{R_{B_x}^2+I_{B_x}^2}\right) - \dfrac{\sum_{n=1}^{N} I_{(2n-1)H_x}\sin(2n-1)\tau}{\sin\tau}\left(\dfrac{R_{B_x}}{R_{B_x}^2+I_{B_x}^2}\right) \end{cases} \quad (4)$$

In the same way, v_{yr} and v_{yi} can be obtained.

2.3 Formulation for Magnetic Analysis

From the Maxwell's equations and the constitutive relation, the governing equation in two-dimensional magnetic field can be written as follows:

$$\frac{\partial}{\partial x}\left(a_4\frac{\partial A_z}{\partial x}-a_3\frac{\partial A_z}{\partial y}+b_4\int\frac{\partial A_z}{\partial x}d\tau-b_3\int\frac{\partial A_z}{\partial y}d\tau\right) + \frac{\partial}{\partial y}\left(a_1\frac{\partial A_z}{\partial y}-a_2\frac{\partial A_z}{\partial x}+b_1\int\frac{\partial A_z}{\partial y}d\tau-b_2\int\frac{\partial A_z}{\partial x}d\tau\right)=J_0+J_m$$
$$\because J_m = \upsilon_0 rotM \quad (5)$$

$$\begin{cases} a_1 = \cos^2(\phi)v_{xr}+\sin^2(\phi)v_{yr} \\ a_2 = a_3 = \sin(\phi)\cos(\phi)v_{xr}-\sin(\phi)\cos(\phi)v_{yr} \\ a_4 = \sin^2(\phi)v_{xr}+\cos^2(\phi)v_{yr} \end{cases} \quad (6)$$

$$\begin{cases} b_1 = \cos^2(\phi)v_{xi}+\sin^2(\phi)v_{yi} \\ b_2 = b_3 = \sin(\phi)\cos(\phi)v_{xi}-\sin(\phi)\cos(\phi)v_{yi} \\ b_4 = \sin^2(\phi)v_{xi}+\cos^2(\phi)v_{yi} \end{cases} \quad (7)$$

where J_0 is the exciting current density, J_m is the magnetization, A_z is the magnetic vector potential and ϕ is the inclination angle between the X-axis and the rolling direction.

2.4 Magnetic Power Loss

In this method, the iron loss can be calculated directly from the vector **B** and the vector **H** by using the following equation.

$$P_t = \frac{1}{\rho T}\int_0^T\left(H_x\frac{dB_x}{dt}+H_y\frac{dB_y}{dt}\right)dt \ \text{[W/kg]} \quad (8)$$

where ρ is the material density and T is the period of the exciting waveform.

3. Machine Construction

Generally, the Power of rotating machines is defined with the following equation.

$$P \propto D_g^{\,2} \times L \times B_g \times AC \times N \quad (9)$$

where D_g is the armature diameter, L is the core length, B_g is the magnetic loading, in other words the air-gap magnetic flux density, AC is the electric loading, in other words the ampere-conductors, N is the rotational speed.

This design was made to increase the magnetic loading within limited volume to take more power. In order to achieve high performance, secondary excitation by the high performance magnets and the grain-oriented electrical steel sheets were selected and a new design making use of dual rotors that are created by an arrangement of permanent magnets on the outer and inner side of the stator core is proposed.

Fig. 5 shows the construction of a high-performance generator. The number of pole is 12. Each rotor was formed with 12 magnets for this 12 poles machine. The permanent magnets are Nd-Fe-B which increase the air-gap magnetic flux density within limited volume. For the winding a single-phase air-gap winding was selected, which is a concentrated winding with high space factor.

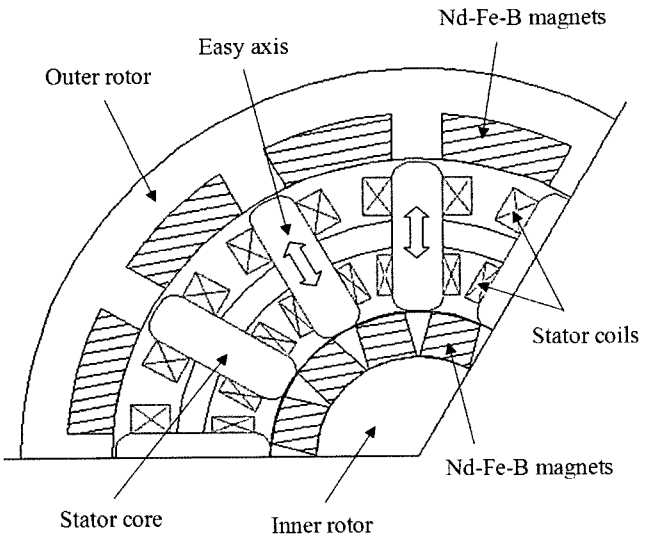

Fig. 5 Construction of Rotating Machine

4. Results and Discussions

Fig. 6 shows the distribution of magnetic flux by using a grain-oriented electrical steel sheet. Fig. 7 shows the loci distribution in stator core of the magnetic flux density vector B and the magnetic field strength vector H. It is evident that the phase difference exists for the relationship between B and H. Fig.8 shows the distribution of iron loss in stator core. From these figures, the rotating magnetic flux has occurred in the outside top of the stator core and the rotating magnetic flux give rise to the increase of the local iron loss. In this analysis we assumed that the magnetic flux density was a perfect sine wave and the eddy current loss was included in the experiment of data.

Fig. 9 shows the distribution of the maximum magnetic flux density B_{max} by using a grain-oriented electrical steel sheet and a non-oriented electrical steel sheet. The non-oriented electrical steel sheet in comparison with the grain-oriented electrical steel sheet has a higher magnetic flux density, and the local concentration of the magnetic flux density is smaller. The performance of the grain-oriented electrical steel sheet was able to be expressed accurately in the analyzed results.

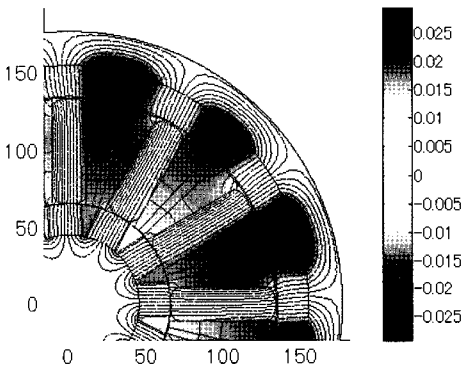

Fig. 6 Distribution of the magnetic flux.

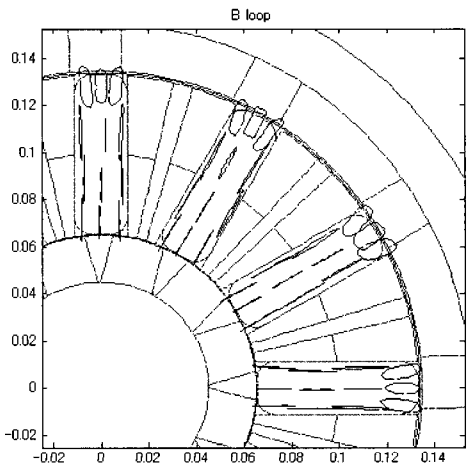

(a) Loci of B

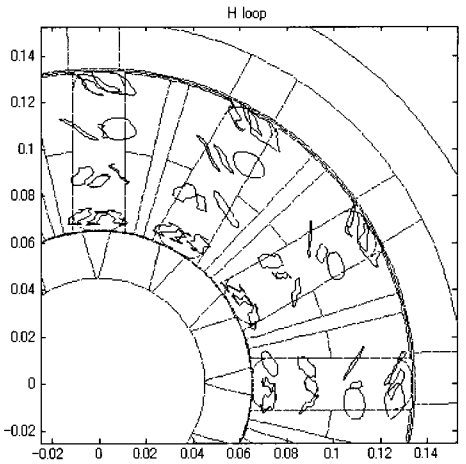

(b) Loci of H

Fig. 7 Distribution of loci of B and H-vector

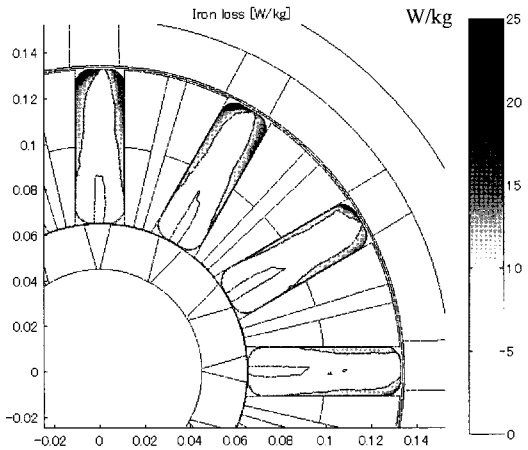

Fig. 8 Iron loss distribution.

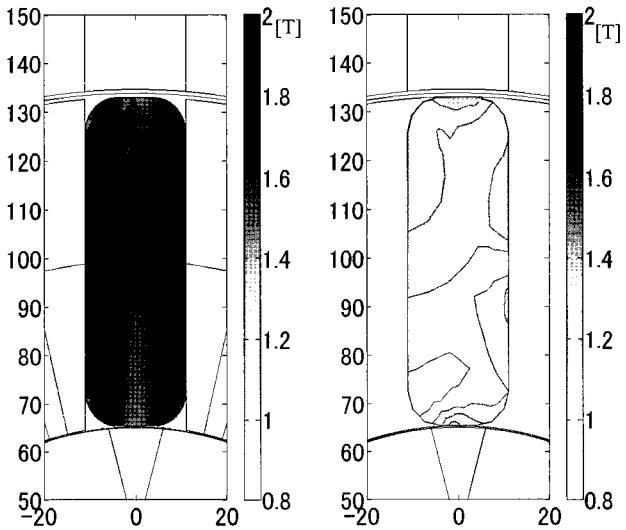

(a) Grain-oriented electrical steel sheet

(b) Non-oriented electrical steel sheet

Fig. 9 Distribution of the maximum magnetic flux density B_{max}.

5. Conclusion

It should be pointed out that the machine is not yet completed and therefore only calculation results have been presented. In this paper, the new modeling of the vector magnetic properties for the nonlinear magnetic field analyses has been presented. It became possible to express the magnetic anisotropy of magnetic material with this modeling.

References

[1] H. Shimoji, M. Enokizono, T. Todaka, T. Honda, "A new modeling of the vector magnetic property," *IEEE Transactions on Magnetics*, Vol. 38, No. 2, pp. 861-864, Mar. 2002.

[2] H. Shimoji, M. Enokizono, T. Todaka, T. Horibe, "New Magnetic Field Analysis Considering a Vector Magnetic Characteristic," *KIEE International Transactions on EMECS*, Vol. 2-B, No. 4, pp. 149-155, 2002.

[3] H. Shimoji, M. Enokizono, "E&S2 model for vector magnetic hysteresis property," *Journal of Magnetism and Magnetic Materials*, Vol. 254-255, pp. 290-292 (2003).

[4] M. Enokizono, T. Todaka, S. Kanao, and J. Sievert, "Two-Dimensional Magnetic Properties of Silicon Sheet Subjected to a Rotating Field," *IEEE Transactions on Magnetics*, Vol. 29, No. 6, pp. 3550-3552, 1993.

[5] M. Enokizono, "Two-Dimensional Vector Magnetic Property," *Journal of the Magnetics Society of Japan*, Vol. 27, No. 2, 2003.